Lab on a Chip

Accepted Manuscript

ROYAL SOCIETY OF CHEMISTRY

www.rsc.org/loc

Journal Name

RSCPublishing

ARTICLE

Bacterial Chemotaxis on SlipChip†

Cite this: DOI: 10.1039/x0xx00000x

Chaohua Shen[a,b], Peng Xu[b], Zhou Huang[b], Dongyang Cai[b], Shuang-jiang Liu[‡b], Wenbin Du[‡b]

Received 00th January 2012,
Accepted 00th January 2012

DOI: 10.1039/x0xx00000x

www.rsc.org/

This paper describes a simple and reusable microfluidic SlipChip device for studying bacterial chemotaxis based on free interface diffusion. The device consists of two glass plates with reconfigurable microwells and ducts, which can set up 20 parallel chemotaxis units as duplicates. In each unit, three nanoliter microwells and connecting ducts could be assembled for pipette loading chemoeffector solution, bacteria suspension, and 1X PBS buffer solution respectively. By simply slipping operation, three microwells were disconnected with other units, and interconnected by the ducts, which allowed the formation of diffusion concentration gradients of the chemoeffector for inducing cells migration from the cell microwell toward the other two microwells. The migration of cells in the microwells was monitored and accurately counted for evaluation of chemotaxis. Moreover, the migrated cells could be easily collected by pipetting for further study after a slip step to reconnect the chemoeffector microwells. The performance of the device was evaluated with chemotaxis of two *Escherichia coli* species, with aspartic acid as the attractant and nitrate sulfate as the repellent. It also enables separation of bacteria species from a mixture based on difference of chemotactic abilities, and collection of cells with strong chemotactic phenomena for further studies off the chip.

INTRODUCTION

Chemotaxis is an important behavior of biological cells that enables them to sense chemical gradients and direct their migration.[1-6] Many cells are guided by chemotactic response towards comfortable colonization sites or away from toxins. For example, chemokine plays an important role in metastasis and angiogenesis;[7] autoimmune inflammatory disorders, like atherosclerosis, are induced by pro-inflammatory cytokines;[8] *Helicobacter Pylori* is guided to the mucus lining of the human stomach,[9] resulting in increased rates of host infection; toluene-degrading *Pseudomonas putida F1* move to the environmental pollutants, which can be exploited for bioremediation.[10]

Study of chemotaxis relies on tools that generate and maintain chemical gradients and monitoring the dynamic distribution of living cells. In recent years, microfluidic technologies have boosted the emergence of various powerful tools for analyzing numerous biological processes,[11-15] including the development of various devices for improving the chemotaxis assays of bacteria and mammalian cells.[15-19] These microfluidic devices can be classified as flow-based methods and diffusion-based methods. The flow-based devices provide well-controlled gradient with stable laminar flow[20]. However, it is difficult to preserve cell autocrine/paracrine secretion in continuous flow systems, which may have impact on cell migration.[21] Chemotaxis of cells in flow is also affected by hydrodynamic shear stress.[22] On the other hand, diffusion-based methods provide flow-free environment by introducing diffusive barriers, such as membrane,[23] self-assembled microspheres[24] or hydrogels,[25] to precisely control chemical diffusion. However, the fabrication and preparation of diffusion barriers remain as technical obstacles for these devices to be widely applied. In addition, current diffusion-based methods are generally not able to selectively harvest the cells of interests.

SlipChips are microfluidic devices which control multiplexed liquid experiments in nanoliter scales by slipping of contacted plates.[26-28] Recently, Various interesting applications have been demonstrated, including protein crystallization,[29] polymerase chain reaction,[30, 31] and immunoassay-based diagnostics.[27] In a device for protein crystallization screening based on free interface diffusion (FID),[29] controllable and variable diffusion concentration gradients were generated for optimization of protein crystal nucleation and growth.[29] Illuminated by this FID design and features, we described in this paper a simple microfluidic SlipChip device which can set up gradient-driven chemotaxis experiments. The diffusion process in the chemotaxis experiment can be initiated or terminated by slipping the device. Chemotactic migrated

bacteria within a given time interval could be collected for off-chip cultivation by pipetting. We introduced a parameter we called the chemotaxis index to evaluate the chemotactic activity of bacterial cells.

MATERIALS AND METHODS

Bacterial strains and materials. Microbial species used are *Escherichia coli* (*E. coli*) RP437 carrying plasmid DsRedT.4 and *E. coli* RP1616 carrying plasmid pACGFP1 (Clontech Laboratories, Mountain View, CA). RP437 and RP1616 without exogenous plasmids were kindly provided by Professor J. S. Parkinson from the University of Utah.[32] The RFP-tagged RP437 and GFP-tagged RP1616 were cultured overnight at 30 ºC in Luria-Bertani (LB) broth containing 100 μg/mL ampicillin. 20 μL overnight cultures were inoculated in 3 mL fresh LB broth and grew for 4 hours at 30 ºC. Cells were collected by centrifugation at 6000 rpm for 3.5 min. The supernatant was discarded and bacteria pellet was suspended in 1X PBS buffer containing 100 μM EDTA. The OD_{600} of bacteria suspension was adjusted to 0.12 for the chemotaxis experiments unless otherwise stated. Solutions of aspartic acid (Asp) with a pH of 7.0 and nickel sulfate (Ni^{2+}) with a pH of 6.5 were prepared in 1X PBS as the attractant and the repellant.

Fabrication of the device. The optimized design of the device in AutoCAD 2006 format was provided in the Electronic supplementary information (ESI). The device was fabricated using two glass plates by standard photolithography and wet chemical etching techniques.[33] Soda-lime glass plates coated with photoresist and chromium were ordered from Telic Company (Valencia, CA). Photomasks were design using AutoCAD (San Rafael, CA) and ordered from MicroCAD photomask Co. Ltd. (Shenzhen, China) The top plate contains microwells and ducts of 60 μm in depth, and the bottom plate glass contains ducts of 20 μm in depth (Fig. 1B). The access holes on the top plate were drilled by a diamond drill bit 0.89 mm in diameter. The glass plates were thoroughly washed with ethanol, oxidized in a plasma cleaner (Harrick Plasma, Ithaca, NY), and silanized by 1H,1H,2H,2H-perfluorooctyltrichlorosilane (Fluorochem Ltd., Derbyshire, UK) in a vacuum desiccator for 4 hours. The glass plates were baked in 65 ºC overnight, rinsed and dried again and kept in a clean Petri dish before use.

Device operation. The two plates of the device were assembled with about 3 μL of fluorinated oil (FC-40, 3M) added on the edge of the device, allowing the oil wetted into the gap between the two glass plates by capillary force in about 10 min, to ensure smooth slipping and prevent leakage.. Aqueous solutions of blue, red and yellow dyes were utilized to demonstrate the operation and diffusion process. First, different solutions were injected into three fluidic paths respectively by pipetting (*state I*, Fig. 1C). Second, the top plate was slipped to the left, form isolated units with three individual microwells connected by two ducts with effective lengths of 418 μm (*state II*, Fig. 1D). In each unit, difference of concentration drove the diffusion between microwells, and a clear diffusion concentration gradient was formed across the ducts. After a certain time period, the top plate was slipped again (*state III*, Fig. 1E), as the 3 microwells in one unit were disconnected and the array of chemoeffector (or buffer) microwells were connected with short ducts for collecting solutions by pipetting. Synchronized tests were conducted in all units simultaneously. After the experiment, the device could be opened and washed with detergent and ethanol, and be reused virtually with no limit on the number of times.

Chemotaxis assays. The device was assembled as described above. A 10 mg/mL bovine serum albumin (BSA) solution was injected in all channels to treat the surface for 30 min prior to the assay to avoid cell adherence. After removing the BSA solution by applying vacuum via the access holes, the chemoeffector solutions were loaded to top microwells, bacteria suspension in PBS to the middle microwells and 1X PBS to the bottom microwells. Excess volume of solutions was injected for flushing out the residue of BSA in the microwells. The device was slipped to the *state II*, during which the cells start to migrate freely from the center microwells to the ducts and microwells loaded with the chemoeffector or PBS. The device was placed on an inverted fluorescence microscope (Ti-Eclipse, Nikon, Japan) and the migration of cells in the presence of the chemoeffector gradient was monitored with timelapse of 5 min. Chemotaxis was evaluated by counting the number of cells in the chemoeffector microwells and PBS microwells at different time points. All the number provided were the average of five parallel units in one experiment. Finally, the device was slipped to *state III*, and the migrated cells was collected for scale-up cultivation.

Numerical Simulation. We used COMSOL Multiphysics (Stockholm, Sweden) to simulate free interface diffusion process in the device. The diffusion coefficient of 4.9×10^{-10} m^2/s was used for fluorescein as the model chemoeffector[18].

RESULTS AND DISCUSSION

System design. Free interface diffusion (FID) based microfluidic devices can precisely control inter-diffusion between microwells connected by narrow ducts, and were used for protein crystallization screening in small volumes.[34] Here, the dynamic diffusion concentration gradient based on FID together with the SlipChip technologies was used for studying bacterial chemotaxis. As shown in Fig. 1, we designed the device contained multiple FID chemotaxis units that were operated in parallel. The basic objective is to precisely control FID among three nanoliter microwells: a microwell (10 nL) to be loaded with bacteria cells in middle, two microwells (16 nL) to be loaded with chemoeffector and 1X PBS buffer. First, we assembled the device as the *state I* and loaded individual solutions in their corresponding microwells. Then the device was slipped to *state II* and the three microwells were connected by the ducts, the concentration difference drove the formation of chemoeffector gradient between the top microwell and the bottom microwell, resulting in the migration of bacteria in the middle microwells towards the top or the bottom microwells

according to their chemotactic preferences. The bacterial cells could freely moving towards or against the FID gradient of the chemoeffector in the device with no shear stress. Because of the three microwells are all on the top plate with fixed distances, and the duct is designed to be much longer and shallower than the microwells, with careful alignments, the FID gradient can be generated very reproducibly for chemotaxis assays. By multiplexing of the design, we can test multiple chemoeffectors or cell types (See supporting information for an optimized design with 4 sets of assays). Furthermore, we can also enhance the device with different duct geometry and microwell volumes to introduce different gradient conditions in an array.

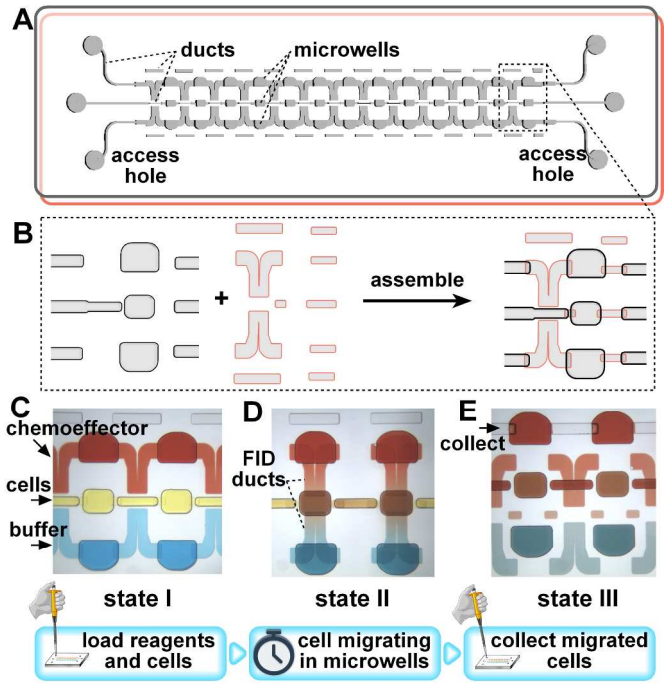

Figure 1. The operation of chemotaxis microfluidic device. (A) Schematic illustration of the device with multiple chemotaxis units. (B) Zoom-in view of the assembly of the top and the bottom plates; (C-E) Step by step operation illustrated by food dyes. The device was loaded with CE (chemoeffector), BA (bacteria) and BF (buffer) at *state I*. After slipping, loading ducts were disconnected from microwells, and created a diffusion concentration gradient for bacterial chemotaxis at *state II*. Afterwards, the device was slipped again to terminate the experiment and collect migrated cells.

Evaluation of the time-dependent diffusion process. To validate the FID process in the device, we used fluorescein as a model "chemoeffector". 100 μM Fluorescein in 1X PBS was loaded into the upper channel and 1X PBS into middle and bottom channels at *state I* and then the device was slipped to *state II* to form experimental units (as shown in Fig. 1C-D), where the fluorescein started diffusing (Fig. 2). As shown in Fig. 2A, the numerical simulation revealed that a steep gradient in the duct toward fluorescein rapidly formed in less than 1 min. As the fluorescein quickly diffused into the middle microwell, a gradient inside the middle microwell are also formed as early as 30 seconds, which means that the cells loaded in the middle microwells were exposed to the gradient of chemoeffector at the very beginning. Spatial and temporal analysis showed that the gradients were mainly distributed on the ducts since they were much shallower than the microwells. The fluorescence reduced gradually in the chemoeffector microwells and increased in the middle microwells and control microwells during the time (Fig. 2C), showing a good agreement between the numerical and the experimental data.

Since it took us about 4~5 min to setup the multi-position imaging on the microscope, the time-lapse fluorescence imaging was started at 5 min. As shown in Fig. 2B, linear gradients of fluorescence intensity was observed in the ducts at 5 min after the ducts connected the microwells. We measured the fluorescence gradient in duct I and duct II as shown in Fig. 2D and 2E. The fluorescence intensities of the microwells and channels were normalized by subtracting the background signals and dividing the initial intensities. The diffusion experiments suggested that the concentration gradient could last for more than 1 hour, which is sufficient for bacteria to make the chemotaxis choice. To provide a more stationary gradient, we could use microwells with bigger volumes for chemoeffector and buffer on two sides, and use shallower ducts to limit the diffusion speed.

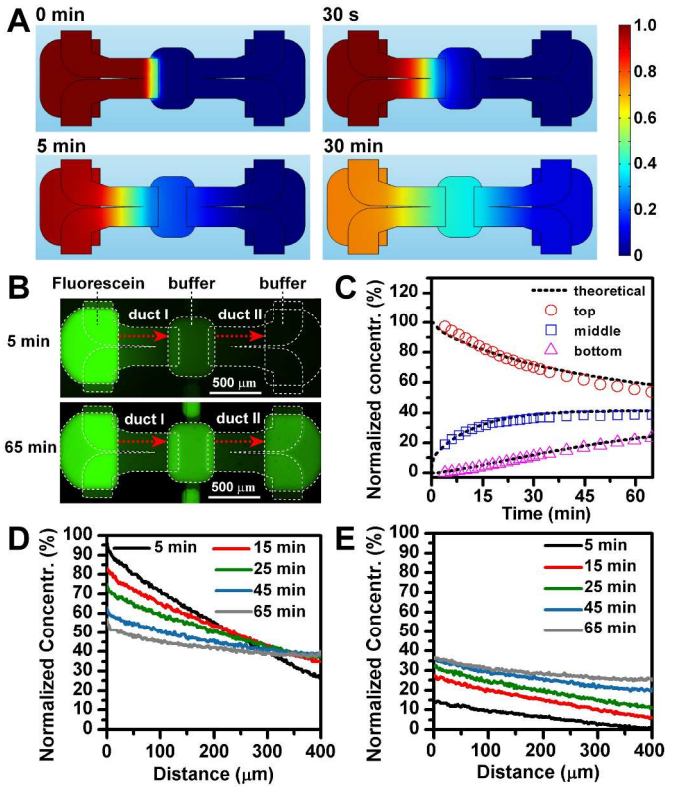

Figure 2. The fluorescence intensity profiles. (A) Numerical simulation of free-interface diffusion of fluorescein; (B) Fluorescence microphotographs at the beginning and 60 min later. The normalized fluorescence intensity profiles of three microwells in 60 min (C), duct I (D) and duct II (E) at different time points along the dot lines.

Measurement of bacterial chemotaxis. It was noticed that time-dependent gradients on the ducts were not sufficient for absolutely quantitative chemotaxis assays since the concentration gradients were dynamically changing. Therefore,

we evaluated chemotaxis of the bacteria based on the number of migrated cells in the microwells containing the chemoeffector or the control buffer in a given time period. To test whether the microfluidic device was suitable for reliable measurement of bacterial chemotaxis, we monitored migration of RP437 in 1 hour with an interval of 5 min starting from 5 min after the slipping operation. We loaded cells (OD_{600} = 0.12) in the middle microwells, and tested it with different chemoeffectors including 200 μM Asp (attractant), 200 μM Ni^{2+} (repellent) and 1X PBS (control) filling the top microwells. As shown in Fig. 3, the attractant Asp, as well as the repellent Ni^{2+} successfully induced obvious bacterial chemotactic responses. At 5 min, cells migrated toward Asp is 10.3 cells with standard deviation of 1.5 cells (expressed as 10.3±1.5), and toward buffer was 1.8±1.7; After 30 min migration, the average number of bacteria in the Asp microwells was 179±11.7, while in the control microwells was 2.8±2.5, which showed an effective attraction of Asp on RP437 (Fig. 3B and 3C). A strong repelling effect of 200 μM Ni^{2+} on RP437 was also observed as shown in Fig. 3D, Cells were swimming in the opposite direction. At 5 min, the cell number in PBS buffer is 56.3±4.0, compare with 0 in Ni^{2+} microwells; At 30 min, the cell number in PBS buffer microwells is 152.2±24.8, compare with 0.3±2.6 in Ni^{2+}. A control experiment was carried out with the chemoeffector microwell and the control microwell both loaded with PBS buffer (Fig. 3E). As a consequence, we found cells in both microwells were increasing at a similar rate, suggesting that no artificial chemotaxis was taken place on the device. These results showed good reproducibility of cell migration in the early beginning (5 min) and during 60 min, indicating the rapid formation of FID gradient provide a sufficient for avoid random migration of cells away from the middle microwells was insignificant.

To evaluate the chemotactic ability of bacterial cells with a chemoeffector at a certain concentration, we introduced a parameter called chemotaxis index, which is simply,

$$I_t = \frac{N_e}{N_e+N_c} \times 100\%$$

where N_e and N_c are the number of cells migrated towards the chemoeffector microwells and the control microwells, and I_t is defined as the number of cells migrated towards the chemoeffector (N_e) divide by all cells migrated (N_e+N_c) in a given time period t. We didn't count the cells in the loading microwell because it also contained dead cells or cells with defects of flagella or motility caused by sample preparation.

I_t is a percentage in between 0% to 100%, and can be used for indicating both positive and negative chemotaxis. In the beginning stage of diffusion, I_t cannot precisely reflect the chemotaxis response because it takes time for the cells to move through the 400 μm ducts and very few cells migrated into the chemoeffector and control microwells were observed. The optimal I_t and its t could be determined according to the diffusion coefficient of the chemoeffector and the motility of the bacterial cells. The value of I_t is approximately equal to 50% if the cells has no response to the chemoeffector. I_t increases to more than 50% if cells are attracted by the chemoeffector, and decrease to less than 50% if the cells are repelled by the chemoeffector. Fig. 3F shows the curve of I_t as a function of time for evaluating chemotaxis of RP437 towards Asp and Ni^{2+}. I_t of RP437 towards Asp is higher than 90% after 10 min, and is around 0% for Ni^{2+}. For control experiments, I_t stayed around 50%.

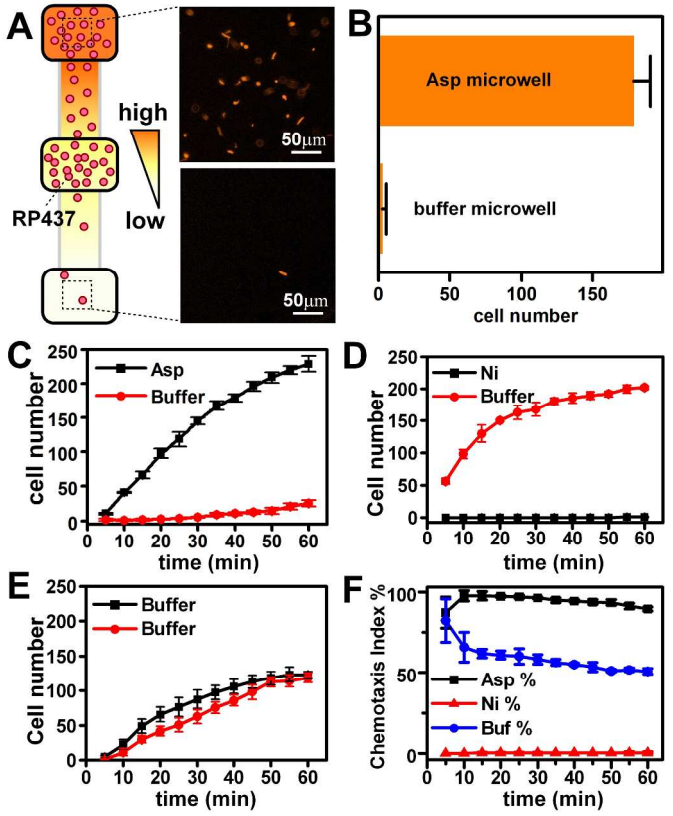

Figure 3. (A) Fluorescence microphotographs shows RP437 migrated into the microwells with Asp, 30 min after FID was initiated. (B) The statistics of cell number in the effector microwells and control microwells in panel A. (C-E) Continuous monitoring of E. coli RP437 migration in experiments with the chemoeffector microwell loaded with Asp, Ni^{2+} and 1X PBS buffer solutions. (F) The temporal tendency of chemotaxis index for Asp, Ni^{2+} and 1X PBS (control)

Based on analysis in the chemotaxis experiments of RP437 on device, we chose I_{30}, which is the chemotaxis index at 30 min, for evaluating its chemotaxis. Once I_{30} was defined as the evaluating parameter of the experiments, we can setup multiple devices simultaneously without monitoring the process of migration, but wait for 30 min for each device, and slipped the devices from *state II* to *state III* under a stereoscope (as shown in Fig. 1E). The devices at *State III* can be stored at 4 ºC if they are not going to be imaged immediately. Migrated cell numbers are counted for the calculation of I_{30} for all devices. Therefore, the device is able to evaluate chemotaxis without relying on timelapse imaging, which is critical for other diffusion-based microfluidic devices for chemotaxis. Utilizing this procedure, the effect of Asp concentration in the range of 0 to 10 mM on chemotaxis of RP437 was studied. As shown in

Fig. 4, RP437 had a strong response (I_{30}>80%) with the Asp concentration from 50 μM to 1 mM. When the concentration of Asp was decreased to 10 μM, I_{30} is 68%, indicating a decrease of efficiency. In general, I_{30} provided valuable information about the speed and intensity of chemotaxis for RP437, which helped us to evaluate how strong a chemotactic response was and what is the range of optimal concentration for the chemoeffector.

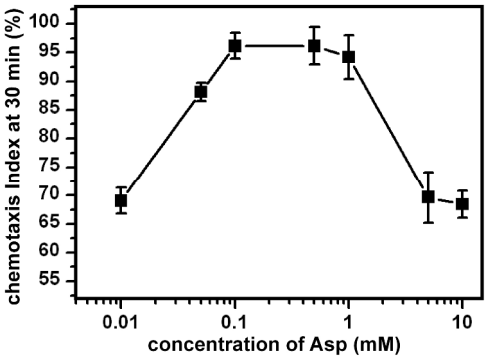

Figure 4. The effect of Asp concentrations on chemotaxis of RP437 evaluated by chemotaxis index at 30 min. each point is the average results from 20 duplicated experiments.

Separation and collection of chemotactic bacteria. The device can selectively separate and enrich bacteria from a mixture based on motilities and chemotaxis responses of different species. This was tested by 1:1 mixture of RP1616 (green) and RP437 (red) as shown in Fig. 5. It has been noted that the strain RP1616 has poor motility and strain RP437 is highly motile towards Asp.[18] Before the test, both bacteria had similar cell number; the ratio of cells for two strains was about 50%. After chemotaxis with Asp for 30 min, a significantly higher number of RP437 were detected in the chemoeffector microwells than RP1616, while in the control microwells, very few cells were collected. Analysis of fluorescence microphotographs indicates that >96% were RP437 and <5% were RP1616 (Fig. 5C). Therefore, the two species were successfully separated.

Furthermore, the chemotactic cells reached at the chemoeffector microwells can be easily collected from the device. As shown in Fig. 5D, after slipping from *state II* to *state III*, the chemoeffector microwells was connected with an array of horizontal ducts and the access holes. The bacterial cells were collected by using a 10 μL pipette. The collected cells are spread onto a LB plate and cultivated overnight. We found that 97% colonies grown from single cells showed red fluorescence and only 3% showed green fluorescence (Fig. 5E), which was consistent with data obtained from cell counting on device.

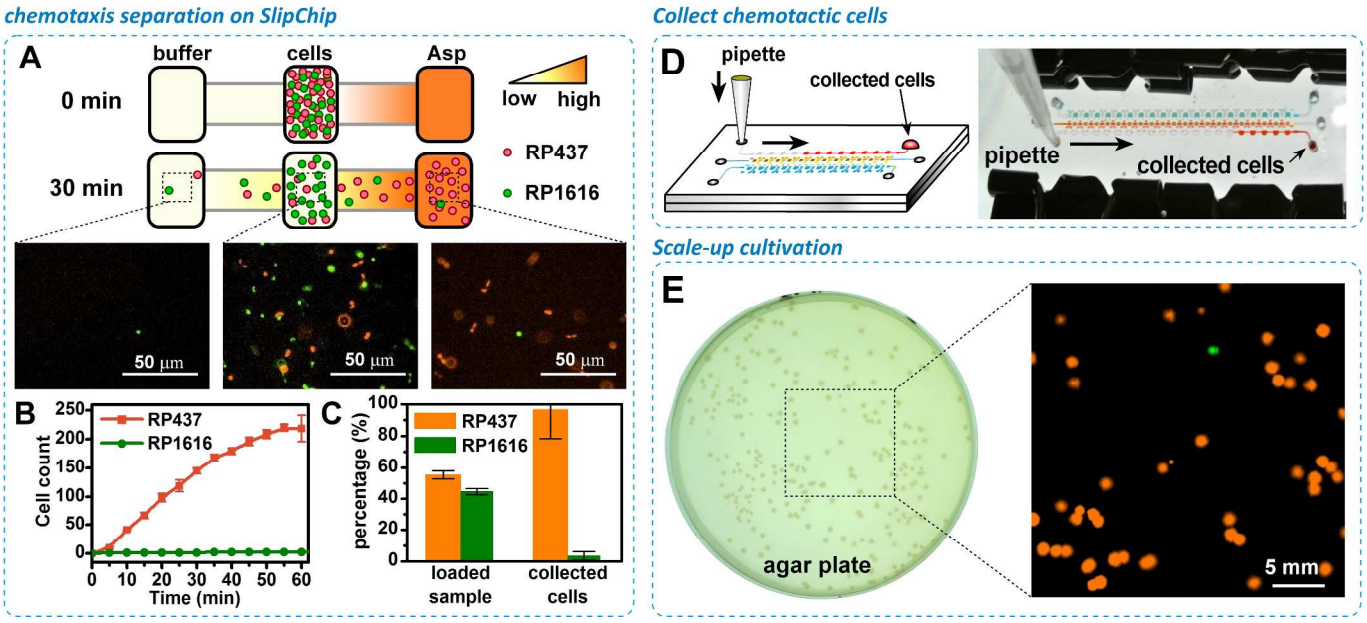

Figure 5. Separation of chemotactic species from a mixture. (A) profile represent the bacteria of RP437 and RP1616 distribution on the device 30min after FID started, with a loaded sample containing E. coli RP437(red) RP1616 (green) at ratio of approximately 1:1; (B) The dynamic migration of RP437 and RP1616 with Asp as the chemoeffector in 1 hour; (C) The counted percentage of two strains before and after 30 min chemotaxis; (D) Chemotactic bacteria were pipetted out of the microwells and collected; (F) Collected bacteria were plated on LB agar for cultivation. The Green/Red fluorescence overlay of the colonies grown from single cells was obtained by the inverted microscope.

CONCLUSION

In this work, we developed a simple microfluidic device for chemotaxis assay and selective enrichment of chemotactic species. The reconfigurable device provides a versatile approach for generating FID concentration gradient of the chemoeffector, evaluating bacteria behavior, and harvesting bacteria of interests. The device can be easily cleaned and reused without further modification. The only consumptive

material is only microliter FC-40 oil for lubricating the slip and prevent leakage. Compared with the existing diffusion-based or flow-based chemotaxis devices, this device has the following advantages: i) it is easy to set up and can generate controllable concentration gradient based on the geometry of the ducts and the microwells; ii) the length and width of ducts can be optimized along with motilities of different cells and diffusion coefficient of different chemoeffectors; iii) by slipping operation, we can initiate or terminate the chemotaxis experiment easily, and an optimal chemotaxis time could be chosen based on experiments and the corresponding chemotaxis index could be utilized for evaluating chemotaxis phenomena; iv) feasible to test attractants and repellents simultaneously, or to investigate the antagonistic effect of both; v) chemotactic bacteria can be selectively isolated in separated microwells by a slip, resulting in the separation of bacteria from a mixture; vi) it enables us to easily harvest bacteria with chemotactic responses by pipetting; vii) very low cost and can be used in common laboratory with no limitation of reuse.

In summary, this device has the merits that it imposing zero shear stress on bacterial cells, performs multiple parallel experiments on-chip requires no external controlling instruments, and generates reliable results. The current device is designed for bacterial chemotaxis assays, and can possibly be extended for studying other cells such as cancer cells or neutrophils. Collectively, the device developed in this work provides a versatile and function-oriented designing capacity to meet the requirement of controllable chemotaxis studies, and a practical workflow for enrichment of chemotactic cells for a variety of applications. The device may also be utilized for isolating bacteria species or subpopulations which have stronger chemotactic response to a certain selected chemical, for directed selection and evolution.

Acknowledgements

This work was supported by: the National Natural Sciences Foundation of China (Grants 21205134, 31230003); the program of China Ocean Mineral Resources R & D Association (Grant DY125-15-R-02); the National High Technology Research and Development Program of China (2012AA092103); the Fundamental Research Funds for the Central Universities, and the Research Funds of Renmin University of China (12XNLI04); State key Laboratory of Microbial Resources, Institute of Microbiology, Chinese Academy of Sciences (Grant SKLMR-20120604).

Notes and references

[a] Department of Chemistry, Renmin University of China, 100872 Beijing, China.
[b] State Key Laboratory of Microbial Resources, Institute of Microbiology, Chinese Academy of Sciences, Beijing 100101, China.
†An Optimized version of AutoCAD design of the SlipChip device for performing four different chemotaxis experiments each with twenty duplicates was provided in the Electronic Supplementary information (ESI), download from DOI: 10.1039/x0xx00000x.

‡ Corresponding author: W. D., wenbin@im.ac.cn; S.L., liusj@im.ac.cn.

References

1. M. Baggiolini, *Nature*, 1998, **392**, 565-568.
2. F. Balkwill, *Nat. Rev. Cancer*, 2004, **4**, 540-550.
3. J. G. Cyster, *Science*, 1999, **286**, 2098-2102.
4. H. Kitano, *Science*, 2002, **295**, 1662-1664.
5. H. Kitano, *Nat. Rev. Genet.*, 2004, **5**, 826-837.
6. A. J. Ridley, M. A. Schwartz, K. Burridge, R. A. Firtel, M. H. Ginsberg, G. Borisy, J. T. Parsons and A. R. Horwitz, *Science*, 2003, **302**, 1704-1709.
7. P. Friedl and K. Wolf, *Nat. Rev. Cancer*, 2003, **3**, 362-374.
8. G. K. Hansson, *J. Thromb. Haemost.*, 2009, **7**, 328-331.
9. M. S. Pittman, M. Goodwin and D. J. Kelly, *Microbiology*, 2001, **147**, 2493-2504.
10. R. E. Parales, J. L. Ditty and C. S. Harwood, *Appl Environ Microbiol*, 2000, **66**, 4098-4104.
11. J. Melin and S. R. Quake, in *Annu. Rev. Biophys. Biomol. Struct.*, 2007, pp. 213-231.
12. H. N. Joensson and H. A. Svahn, *Angew Chem Int Edit*, 2012, **51**, 12176-12192.
13. M. Wu, S. Huang and G. Lee, *Lab Chip*, 2010, **10**, 939-956.
14. T. M. Keenan and A. Folch, *Lab Chip*, 2008, **8**, 34-57.
15. S. Kim, H. J. Kim and N. L. Jeon, *Integr. Biol.*, 2010, **2**, 584-603.
16. T. Ahmed, T. S. Shimizu and R. Stocker, *Integr. Biol.*, 2010, **2**, 604-629.
17. J. Wu, X. Wu and F. Lin, *Lab Chip*, 2013, **13**, 2484-2499.
18. G. Si, W. Yang, S. Bi, C. Luo and Q. Ouyang, *Lab Chip*, 2012.
19. C. Beta and E. Bodenschatz, *Eur. J. Cell Biol.*, 2011, **90**, 811-816.
20. H. B. Mao, P. S. Cremer and M. D. Manson, *Proc. Natl. Acad. Sci. U. S. A.*, 2003, **100**, 5449-5454.
21. C. Beta, T. Fröhlich, H. U. Bödeker and E. Bodenschatz, *Lab Chip*, 2008, **8**, 1087-1096.
22. G. M. Walker, J. Q. Sai, A. Richmond, M. Stremler, C. Y. Chung and J. P. Wikswo, *Lab Chip*, 2005, **5**, 611-618.
23. J. P. Diao, L. Young, S. Kim, E. A. Fogarty, S. M. Heilman, P. Zhou, M. L. Shuler, M. M. Wu and M. P. DeLisa, *Lab Chip*, 2006, **6**, 381-388.
24. E. Choi, H. Chang, C. Y. Lim, T. Kim and J. Park, *Lab Chip*, 2012, **12**, 3968-3975.
25. T. Ahmed, T. S. Shimizu and R. Stocker, *Nano Lett.*, 2010, **10**, 3379-3385.
26. W. B. Du, L. Li, K. P. Nichols and R. F. Ismagilov, *Lab Chip*, 2009, **9**, 2286-2292.
27. Y. Song, Y. Zhang, P. E. Bernard, J. M. Reuben, N. T. Ueno, R. B. Arlinghaus, Y. Zu and L. Qin, *Nat. Commun.*, 2012, **3**, 1283.
28. H. Liu, X. Li and R. M. Crooks, *Anal. Chem.*, 2013, **85**, 4263-4267.
29. L. Li, W. B. Du and R. F. Ismagilov, *J. Am. Chem. Soc.*, 2010, **132**, 112-119.
30. F. Shen, W. B. Du, E. K. Davydova, M. A. Karymov, J. Pandey and R. F. Ismagilov, *Anal. Chem.*, 2010, **82**, 4606-4612.
31. F. Shen, B. Sun, J. E. Kreutz, E. K. Davydova, W. Du, P. L. Reddy, L. J. Joseph and R. F. Ismagilov, *J. Am. Chem. Soc.*, 2011, **133**, 17705-17712.
32. J. S. Parkinson, *J. Bacteriol.*, 1978, **135**, 45-53.

33. Q. H. He, S. Chen, Y. Su, Q. Fang and H. W. Chen, *Anal. Chim. Acta*, 2008, **628**, 1-8.

34. C. L. Hansen, E. Skordalakes, J. M. Berger and S. R. Quake, *Proc. Natl. Acad. Sci. U. S. A.*, 2002, **99**, 16531-16536.